Ongoing Developments in the use of Continuation-Bifurcation Methodology at AgustaWestland

Mark Jones
Rotor Dynamics and Loads, AgustaWestland
mark.jones@agustawestland.com
Andrea Bernascone
Rotor Dynamics and Loads, AgustaWestland
andrea.bernascone@agustawestland.com
Pierangelo Masarati
Dipartimento di Ingegneria Aerospaziale,
Politecnico di Milano, 20156 Milano, Italy
pierangelo.masarati@polimi.it
Giuseppe Quaranta
Dipartimento di Ingegneria Aerospaziale,
Politecnico di Milano, 20156 Milano, Italy
giuseppe.quaranta@polimi.it
Djamel Rezgui
Department of Aerospace Engineering,
University of Bristol, BS8 1TR, UK
djamel.rezgui@bristol.ac.uk

ABSTRACT

The use of continuation and bifurcation methods in the assessment of stability allows for a complete non-linear stability picture to be gained and also allows for rapid exploration of a multi-parameter space which can be much more efficient than using traditional techniques. In recent years AgustaWestland, the University of Bristol and the Politecnico di Milano have jointly produced and validated interfaces between a well-validated off-the-shelf continuation and bifurcation tool and various in-house AgustaWestland aeroelasticity tools. One piece of software which has been successfully coupled to the tool is the Modern Aeroservoelastic State-Space Tools developed at the Politecnico di Milano. The Modern Aeroservoelastic State-Space Tool is a suite of tools developed in the Matlab/Simulink environment providing the ability to rapidly assemble a complex non-linear dynamic system in the state-space form allowing for the multi-disciplinary study of aeroservoelastic stability and control. The main focus of this paper is to demonstrate the maturity of the tool using as an example its first practical application which contributed evidence towards the latest Release-To-Service of the AW159/Wildcat. Whilst this study does not use the full potential of the continuation and bifurcation methods, it clearly demonstrates the maturity of a non-linear stability analysis capability at AgustaWestland allowing it to be integrated into the every-day suite of tools available to the dynamics engineers.

1 NOTATION

d_{sm}	smoothing parameter
F_{con}	control system force
K_1	control stiffness in backlash region
K_2	control stiffness with bush restraint
x_{bl}	backlash magnitude
Δz_A	control system displacement

Abbreviations:

AW	AgustaWestland
CSA	Coupled Stability Analysis
LCO	Limit Cycle Oscillation
MASST	Modern Aeroservoelastic State Space Tools
C-B	Continuation and Bifurcation

2 INTRODUCTION

The use of continuation and bifurcation (C-B) methods in the assessment of stability allows for a complete stability picture to be gained of systems with significant non-linearity. Furthermore, the continuation method allows for rapid exploration of a multi-parameter space which can be much more efficient than using traditional techniques.

In the aerospace sector, the use of bifurcation and continuation tools is becoming more widespread. In particular, it is increasingly adopted to investigate nonlinear aircraft flight dynamics and control problems. However, the application of continuation and bifurcation methods has been limited to a small number of helicopter dynamical problems, such as flight mechanics[1–7], ground resonance[8,9], and examination of rotor vortex ring state[10]. Researchers at the University of Bristol (UoB) have been investigating the use of C-B methods in the field of rotorcraft for several years. In recent years, under the banner of the AgustaWestland/University of Bristol University Technology Centre (UTC), interfaces between a well-validated off-the-shelf C-B tool and various in-house AgustaWestland (AW) aeroelasticity software have been produced. These coupled tools have been previously demonstrated and validated against legacy stability analysis tools[11-13]. Example case studies included: nonlinear aeroelastic blade stability, blades with trailing edge flaps and rotors with non-linear pitch-link stiffness.

One of the tools with which the C-B software has been successfully coupled is the Modern Aeroservoelastic State-Space Tools (MASST)[14] developed at the Politecnico di Milano (POLIMI). MASST is a suite of tools developed in the Matlab/Simulink environment providing the ability to rapidly assemble a complex non-linear dynamic system in the state-space form allowing for the multi-disciplinary study of aeroservoelastic stability and control. Where appropriate some components of the model are linearised with respect to the system states in the interest of efficiency whilst any non-linear variation with the system parameters is achieved using a variety of advanced interpolation techniques. On the other hand, where there is significant non-linearity with respect to the system states the behaviour is maintained within the model providing the possibility for non-linear assessment. This makes MASST an ideal candidate for coupling with a C-B tool and therefore an off-the-shelf program has been coupled to MASST by POLIMI with close co-operation from AW and UoB.

The coupled C-B/MASST tool has now reached sufficient maturity such that in the past year it has been used for the first time in a practical, non-research, application. Indeed the analysis performed has contributed evidence towards the latest Release-To-Service (RTS) of the AW159/Wildcat aircraft.

The present paper puts focus on this initial application of the C-B/MASST tool, using the example to explain the processes involved and to demonstrate the analysis which may be performed. By doing so it clearly demonstrates the maturity of a non-linear stability analysis capability at AW allowing it to be integrated into the every-day suite of tools available to the dynamics engineers.

3 CONTINUATION AND BIFURCATION METHODS

The continuation method describes the technique where a parameter of the dynamic system is varied continuously and the steady solutions obtained. Simultaneously, the stability of the solution is assessed using either Eigen or Floquet analysis (depending on whether it is an equilibrium or periodic condition). A bifurcation point is said to occur when the stability of the system changes, thus these points may be detected through inspection of the Eigenvalues (or Floquet multipliers). In a non-linear system the bifurcation points may give rise to new branches. These new branches can then be followed in turn in order build up a full picture of the dynamic behaviour of the non-linear system. For more information on continuation/bifurcation methods the reader is referred to references[15, 16].

Presently at AW, use is being made of the continuation-bifurcation software AUTO[17,18]. In addition to the original Fortran version, use is also being made of the Dynamical System Toolbox which integrates the program into the Matlab environment[19]. AUTO is capable of performing continuation-bifurcation analysis of systems which can be written in the standard first-order ordinary differential equation form. Since MASST may be used to assemble and then export the non-linear system equations in this form the coupling of the two tools is relatively straight-forward as described in the following sections.

4 ASSEMBLY OF A NON-LINEAR ROTOR MODEL

The process of assembling the non-linear model using the AUTO-MASST tool is described here. The AUTO-MASST method was developed in reference[20] and a graphical description of the concept may be seen in Figure 1. The two main components of the tool are of course AUTO and MASST but they are coupled together using the AUTO-MASST set of tools as shown in the diagram. The following sections describe the process in more detail using the present AW159 tail rotor model as an example, although of course the process is generic and applicable to any model which may be assembled in the MASST environment.

4.1 Generation of the Rotor files for the MASST Model

A model of the rotor is first assembled in the comprehensive rotor program Camrad/JA[21]. As the non-linear control system is to be modelled in the Simulink environment, all control system stiffness in Camrad/JA is set to zero and the kinematic (pitch-flap) coupling is also set to zero. A matrix of cases is then run to cover the range of collective and rotor speed values of interest, with spacing between cases to allow a reasonable linear interpolation. In the current study all assessment was done in the hover condition at minimum density altitude and minimum temperature, these conditions being identified during linear analysis to be the most critical. Our main concern here is the coupling between the fundamental flap and pitch modes, but to ensure that any additional coupling with the surrounding modes is taken into account the fundamental lag and first beam bending modes have also been included in the analysis. As some flexibility is included in the first coupled pitch/torsion mode shape the first flexible torsion mode is included in the Camrad/JA analysis as well as the rigid pitch mode. For a single blade the rotor model therefore has five modes of which only the first four are of a real interest, as the last is the second torsion mode which is of much higher frequency. The Camrad/JA output files are then used to generate MASST rotor files using a script provided as part of the MASST package.

4.2 Additional Modifications to the System Matrices

At this stage four modifications were made to the rotor system matrices to account for effects not included in the Camrad/JA model. All modifications were made by editing the MASST rotor files.

4.2.1 Control System Inertia

The inertia of the control system can have a significant contribution to the inertia of the modes of interest. This effect has been added to the model through appropriate modification of the rotor system mass matrix.

It is noted here that the rotor matrices exported from Camrad/JA are in the multi-blade format, however in the current AUTO-MASST method we will consider only a single blade, isolated rotor analysis (in order to minimise the number of states). Therefore since we will be neglecting any coupling with the fixed-frame the collective, cyclic and reactionless modes obtained from the Camrad/Ja model will be the same (if given the same control stiffness). As we wish to assess only a single blade the choice of using the collective, cyclic or reactionless modes is arbitrary as the same results will be obtained in the rotating-frame. Since the multi-blade matrix elements for the collective and reactionless modes demonstrate a closer resemblance to their equivalent, single blade, modes it is easier to interpret and modify these modes in the manner required by the modification discussed above. Therefore the reactionless modes were chosen and thus the corrections were only applied to the reactionless elements of the mass matrix. Of course all correction terms needed to be multiplied by the number of blades before being added to the multiblade co-ordinate matrices.

4.2.2 Pitch-Flap Inertia Coupling

The Coriolis effect leads to additional inertia coupling appearing in the damping matrix. These terms arise due to any mass located out-of-plane of the rotor disc, as any pitch motion will result in a chordwise deflection of this mass which, through the Coriolis effect, leads to a coupling with the flap mode. These terms can clearly influence the pitch-flap coupling of the fundamental modes if the control system stiffness is low enough. These coupling terms are not included in Camrad/Ja as the out-of-plane inertia component is neglected and so the effect due to these terms is included here through a correction to the system damping matrix.

4.2.3 Lag Damper

For some tail rotors the lag damper can have a significantly stabilising influence on the pitch-flap stability behaviour, this having been previously found to be the case for the AW189 tail rotor. However, for the AW159 tail rotor it is less important to include the damper since the attachment of the damper rod at the feathering axis of the blade means it has minimal influence over the pitch-flap stability. Nevertheless, the damper has been included here to ensure that the lag mode is appropriately damped thus eliminating the possibility that unrealistic bifurcations occurring in that mode might complicate the analysis. Here, the effects due to the damper have been included by adding the equivalent modal stiffness and damping to the matrices.

4.2.4 Structural Damping

It has been found previously from analysis of flight test data that the aeroelastic models of the AW159 tail rotor are conservative in the prediction of the pitch mode damping. Therefore to account for this difference the appropriate amount of structural damping has been added to the pitch mode through modification of the damping matrix.

4.3 Assembly and Export of the Linear Model from MASST

Having generated the rotor system matrices, a Simulink model which uses them as a database is then assembled using MASST. The current AW159 tail rotor model incorporates the following components:

- A very stiff fuselage component with high stiffness, low mass and small but non-zero damping.
- A rotor database including all rotor files generated as described in the previous section.
- A connection to attach the rotor to the fuselage.
- Pitch and flap sensors supplying the inputs used to calculate the displacement at the pitch horn which form the input to the non-linear control system model.
- Pitch and flap external forces which apply the control moments resulting from the reaction force from the non-linear control system model.
- A linear control system which temporarily connects the inputs from the sensors to the external forces using a simple gain. This simple connection is later replaced by the non-linear control system in the Simulink environment.

To simplify the analysis and to keep the number of states to a minimum a single blade analysis is performed and therefore, as discussed above, only the reactionless modes are activated in the MASST environment. Once the MASST model was assembled it was exported to Simulink using a function included as standard in MASST.

4.4 AUTO-MASST Pre-Process Script

Having assembled and exported the model from MASST, a pre-process script is run to complete the assembly of the Simulink model. The script has two main purposes. Firstly, it assembles a Matlab database (written to a .mat file) which contains the set of state-space systems for the discrete set of rotor parameters (the values for which the Camrad/JA simulations were performed) in a format suitable for efficient interpolation. Secondly, it generates an S-function whose purpose is to take as inputs the desired rotor parameters and then to supply the appropriate state-space system by using the MASST interpolation routines along with the previously generated database.

The final stage in the model assembly process is the replacement of the linear control system exported by MASST with the desired non-linear description of the control path, this being defined using an Embedded Matlab Function. For the current model this function has been derived based on test data and is described in detail in the following section.

A screenshot of the final Simulink model is shown in Figure 2. Note that after this stage the only two files required to run the model are the Simulink model itself and the Matlab database file containing the system data for interpolation. The three model parameters which are to be passed to the model by AUTO can be clearly seen in the screenshot and are the RPM (rotor speed), collective pitch, and magnitude of wear on the control system. The S-function block then takes the RPM and collective for interpolation using the MASST routines and couples the system to the non-linear control system definition using the pitch and flap position sensors and external forces/moments.

4.5 Definition of the Non-Linear Cyclic Control System

As stated above, the linear control system generated by MASST needs to be replaced by a representative non-linear form in the Embedded Matlab Function. A schematic of the control system to be represented is shown in Figure 3. The cyclic stiffness is dominated by bending of the actuator output shaft and therefore the bush constraint serves to increase the stiffness. However, the constraint is not ideal, there being a small amount of backlash between the shaft and the bush such that in the backlash region the effective stiffness is reduced. The effect of this backlash can of course increase if the bush were to wear through the life of the component. The non-linearity due to the backlash is represented here using the generalised model shown in Figure 4 where Δz_A is the displacement at the end of the pitch link and F_{con} is the reaction force.

Assume to begin with that d_{sm} is zero such that the format is a bilinear stiffness where the change in stiffness occurs at the backlash magnitude, x_{bl}. The first stiffness (the gradient of the line for $\Delta z_A < x_{bl}$) will be denoted as K_1 and represents the stiffness within the backlash region where the actuator push rod is not being supported by the bush. The second stiffness (the gradient of the line for $\Delta z_A > x_{bl}$) will be denoted as K_2 and represents the system stiffness outside of the backlash region where support is being provided by the bush. Both K_1 and K_2 are assumed to vary with the collective pitch setting, however they are assumed to be independent of the magnitude of the backlash, x_{bl}. Through the life of the component some wear might be anticipated on the bush. Whilst this would not be expected to significantly alter the values of K_1 and K_2, the magnitude of the backlash, x_{bl}, would be increased. Finally, the parameter d_{sm} is used to apply a quadratic smoothing to the change in gradient from K_1 to K_2. This is done to aid the non-linear stability assessment tool, AUTO. In practice d_{sm} can simply be set to a very small value, the precise value having negligible influence on the results so long as it is much smaller (at least an order of magnitude) than x_{bl}.

The bilinear shape used for the generalised model is validated using data obtained from stiffness tests with the bush machined to various diameters to simulate the effect of through-life wear on the bush component. Using this data the values for K_1, K_2 and x_{bl} are set as linear functions of collective pitch and wear. The test was designed to provide the required force-displacement curves (as measured at the end of the spider arm) when the system was put under cyclic loading. The test was carried out with the bush in its nominal (zero wear) configuration, with an intermediate level of wear and finally with a high level of wear. Actuator push rod extensions equivalent to minimum collective and an intermediate collective were considered.

The loads and displacements were measured at both spider arms relevant to the cyclic loading. These measured quantities were then averaged over the two arms to enable the construction of a single force-displacement curve for each value of bush wear for the intermediate and minimum collective cases. The general non-linear model was then fit to the data using selected values of K_1, K_2 and x_{bl}. An example for the nominal clearance at minimum collective is shown in Figure 5.

Such a fit was performed for each clearance (bush wear) case at each collective. The resulting values of K_1, K_2 and x_{bl} were then used to set up a continuous model of these parameters as functions of collective and bush clearance. As stated above the values of K_1 and K_2 were assumed to be independent of the bush wear, being approximated as inversely proportional to the shaft extension (itself a linear function of collective). The value of x_{bl} was assumed to be proportional to the clearance (the bush inner diameter minus the shaft outer diameter) and also a linear function of collective. The fit of this model to the data extracted from the test results is shown for the stiffness and backlash in Figure 6 and Figure 7 respectively.

This model has been incorporated into the Embedded Matlab Function representing the control system in the simulink model. These cyclic stiffness values have been combined with a reactionless value to give the total cyclic control chain stiffness. In order to obtain the correct kinematic coupling, the pitch horn displacement is calculated from the flap and pitch displacements using the appropriate pitch horn geometry. Similarly the control pitch and flap moments are also derived from the reaction force using the same geometry.

5 EQUILIBRIUM (LINEAR) RESULTS

The equilibrium branches should first be calculated. Equilibrium branches are equivalent to the traditional linear stability assessment in that the stability of the branch tells us, for an infinitesimal perturbation, whether the solution returns to or is repelled from the branch. Being equivalent to a linear system, the eigenvalues obtained for the branch can be used to validate the model against the existing data from our traditional linear assessment tools, in this case results from the AW Coupled Stability Analysis (CSA) tool. Having calculated the equilibrium branches and found any bifurcation points we can then trace any secondary branches originating from these bifurcation points to find additional branches of interest.

5.1 Validation of the Model Using Zero Backlash Case (Stiffness=K_1)

The model is first validated by selecting a single control stiffness value and comparing the equilibrium results with those from a standard linearised stability tool, in this case CSA. In order to validate the model a collective sweep was performed at the nominal rotor speed and with the control stiffness equal to the value with no bush restraint (i.e. K_1). The results are in good agreement with CSA as shown in Figure 8. There is some difference in the prediction of the precise location of the stall, but this is not critical for the current investigation as will be seen below.

Further validation is done by performing a variation of the rotor speed, again using the stiffness value K_1. The agreement with CSA is very good as shown in Figure 9, thus we can have significant confidence in the model.

Now we can use the AUTO-MASST model to perform continuations on the rotor speed and collective pitch parameters. Using the continuation program to do this is very efficient with hundreds of conditions being calculated within a matter of seconds. In this way we can fully explore the design space in an efficient manner identifying the critical regions which can then be confirmed using the traditional approach. Therefore, even though this stage does not give any more information than the linear analysis it is already advantageous purely from the efficiency viewpoint.

These continuations were first performed with the control stiffness set equal to K_2. The contours of pitch mode damping ratio provided by these continuation runs are shown in Figure 10. This case represents the system with an ideal bush restraint in place (i.e. with zero backlash). Clearly the critical region in terms of collective angle lies between around -9 to 12 degrees where the highest lift slope is present before the effects due to stall start to occur. Even in this region it can be seen that the rotor remains stable up to rotor speeds beyond the maximum steady power-off value (the stability boundary is given by the 0% contour line). Therefore with an idealised restraint the rotor would remain stable through its operating range.

Consider now the contour for the lower control stiffness, K_1, as shown in Figure 11. Clearly, even in this case the system still remains stable up to rotor speeds slightly above the normal operating value. This is an important result, since it shows that the system is linearly stable at the normal operating rotor speed even without bush restraint and therefore a limit cycle oscillation (LCO) would not be encountered at the normal power-on rotor speed regardless of the level of bush wear. However, the maximum steady power-off rotor speed lies beyond the stability boundary and therefore in this region the rotor can be expected to enter a LCO, albeit one that is quickly bounded by the presence of the bush outside the backlash region.

In summary, the linear results show that since the system is linearly stable without any restraint at the normal operating rotor speed, bush wear will have no effect on stability at this speed and therefore a LCO will not be encountered. On the other hand at power-off rotor speeds, since the system is linearly unstable without the bush restraint, a LCO will be encountered with the magnitude being a function of the size of the backlash region and therefore the bush wear. The magnitude of these LCOs are investigated in the next section.

6 NON-LINEAR CONSIDERATIONS

Since we have found from the linear results that in the presence of backlash the system will enter a LCO in power-off conditions, in this section the magnitude of these oscillations will be investigated for the most critical value of collective as decided based on Figure 11. Varying the rotor speed at this critical value of collective pitch using the continuation software results in the prediction of a Hopf bifurcation at the rotor speed at which the pitch mode goes unstable. At this point an additional branch is created in addition to the equilibrium one, and this branch is periodic with the period approximately equal to the natural frequency of the pitch mode. We can use the continuation software to follow this branch for further increases in rotor speed. In this way the software provides information about how the LCO varies and therefore we can, in a very efficient manner, plot out the variation of the magnitude of the limit cycle against rotor speed without having to perform a time simulation at every point of interest. Of course we can also do this for various values of bush clearance to assess the affect of wear on the LCO.

As output, the software provides the oscillation information for each state, which can be used to calculate the control displacement and therefore the control load. We can directly compare the magnitude of this load, as the LCO varies with rotor speed and bush clearance, with the values used as monitor limits in telemetry during the development flying of the AW159.

6.1 LCO magnitude with the nominal bush clearance

A continuation on the rotor speed parameter was first conducted for the periodic branch with the clearance set to the nominal value. This case therefore represents the LCO which would be encountered in the as-manufactured condition.

The LCO magnitude, in terms of the control load (pitch link force) is plotted versus rotor speed as the black line in Figure 12. Also plotted are blue lines showing the various rotor speeds and red lines showing the various monitor limits. At the max steady power-off rotor speed (dashed blue line) the LCO is clearly well below the 50hr limit (bottom, dot-dash red line). Therefore in the as-manufactured condition the backlash present in the system will not give rise to any damaging loads.

6.2 Variation of LCO magnitude with bush wear

If the bush was to wear through its service life the clearance between the bush and the actuator output shaft increases and therefore the LCO can be expected to increase in amplitude. In this section the continuation software was used to follow the periodic branch (the LCO) whilst the clearance value was increased. This was done with the rotor speed constant at the max steady power-off value.

The results are shown in Figure 13. As the clearance is increased the amplitude increases as expected. However, the 50hr limit is only reached for a clearance value which is far beyond the allowable value (plotted as full blue line). Indeed at the maximum allowable value the amplitude has only a relatively small increase in comparison to the nominal one.

6.3 LCO magnitude with the maximum acceptable bush clearance

Finally, for clarity, the LCO magnitude versus rotor speed is calculated for the bush clearance equal to the maximum allowable. The result is shown in Figure 14. As suggested by the previous plots the magnitude at the max steady power-off rotor speed is below the 50hr limit. This suggests that as long as the bush wear remains within the maximum allowable value then the LCO response will not result in loads of a damaging magnitude. This conclusion provides evidence that the bush maintenance/inspection procedures are sufficient to ensure that the tail rotor dynamic response will remain satisfactory through the life of the tail rotor.

7 FUTURE APPLICATIONS

The AUTO-MASST coupling has been shown during its initial application to be an efficient means of assessing the dynamics of the rotor system when coupled with significantly non-linear components. Having gained confidence with the tool, future applications will consider systems whose non-linear behaviour are less easy to predict. However, by producing bifurcation diagrams clear insight can be provided into the global dynamic behaviour, which might be missed using traditional linear and time simulation analyses. Such applications include the influence of non-linear damper characteristics on rotor-airframe coupled responses along with the influence of flight control software on whirl flutter stability. The ability of the AUTO-MASST framework to rapidly couple the rotor system with a complex non-linear control component makes it ideally suited for such assessments.

8 CONCLUSIONS

- Research into the application of continuation/bifurcation methods to the dynamic study of rotor aeroelastic systems has been the subject of ongoing collaboration between AgustaWestland and the University of Bristol.
- Most recently, further collaboration has been made with the Politecnico di Milano in order to couple a continuation/bifurcation tool to the Modern Aeroservoelastic State Space Tools.
- The result is an industrialised framework which has enabled AgustaWestland to rapidly assess the non-linear dynamic

behaviour of a production tail rotor thus contributing to its release to service.
- The current application has provided confidence and experience with the tool and paves the way towards its application to system components which exhibit more complex non-linear dynamic behaviour.

9 COPYRIGHT STATEMENT

10 REFERENCE DOCUMENTS

[1] Sibilski, K., "Bifurcation Analysis of a Helicopter Non-Linear Dynamics," Archive of Mechanical Engineering, Vol. 46, No. 2, 1999, pp. 171–192.

[2] Sibilski, K., "Nonlinear Flight Mechanics of a Helicopter Analysis by Application of Continuation Methods," 25th European Rotorcraft Forum, Paper H4, Rome, Italy, 1999.

[3] Sibilski, K., "A Study of the Flight Dynamics Helicopter Carrying an External Load Using Bifurcation Theory and Continuation Methods," Journal of Theoretical and Applied Mechanics, Vol. 41, No. 4, 2003, pp. 823–852.

[4] Bedford, R. G., and Lowenberg, M. H., "Use of Bifurcation Analysis in the Design and Analysis of Helicopter Flight Control Systems," 29th European Rotorcraft Forum, Paper 32, Friedrichshafen, Germany, 2003.

[5] Bedford, R., and Lowenberg, M., "Bifurcation Analysis of Rotorcraft Dynamics with an Underslung Load," AIAA Atmospheric Flight Mechanics Conference, Vol. 1, Providence, RI, 2004, pp. 595–619. doi:10.2514/6.2004-4947.

[6] Bedford, R. G., and Lowenberg, M. H., "Flight Dynamics Analysis of Periodically Forced Rotorcraft Model," AIAA Atmospheric Flight Mechanics Conference, Vol. 2, Keystone, CO, 2006, pp. 1210–1228. doi:10.2514/6.2006-6634

[7] Maradakis, G., "Fundamental Nonlinear Characteristics of Helicopter Flight Mechanics," M.S. Thesis, Dept. of Applied Mathematics, Glasgow Caledonian University, Glasgow, 2000.

[8] Mokrane, A., "Helicopter Ground Resonance Prediction Using an Integrated Nonlinear Model," Ph.D. Dissertation, Dept. of Aerospace Engineering, University of Bristol, Bristol, U.K., 2011.

[9] Avanzini, G., and De Matteist, G., "Effects of Nonlinearities on Ground Resonance Instability," 34th European Rotorcraft Forum, Paper No. 10a3, Vol. 3, Liverpool, U.K., 2008, pp. 2327–2378.

[10] Basset, P. M., and Prasad, J., "Study of the Vortex Ring State using Bifurcation Theory," 58th Annual Forum of the American Helicopter Society, Paper No. 167, Montreal, Canada, 2002.

[11] D. Rezgui, M. Lowenberg, M. Jones, C. Monteggia, "Towards Industrialisation of Bifurcation Analysis in Rotorcraft Aeroelastic Problems", In Proceedings of the American Institute of Aeronautics and Astronautics: AIAA Atmospheric Flight Mechanics Conference, 2012.

[12] D. Rezgui, M. Lowenberg, M. Jones, C. Monteggia, "Application of Continuation and Bifurcation Methods to Aeroelastic Rotor Blade Stability", In Proceedings of the 37th European Rotorcraft Forum, Gallarate, Italy, 2011.

[13] D. Rezgui, M. Lowenberg, M. Jones, C. Monteggia, "Continuation and Bifurcation Analysis in Helicopter Aeroelastic Stability Problems", AIAA Journal of Guidance, Control and Dynamics, Vol. 37, No. 3, 2014, pp. 889-897. doi: 10.2514/1.60193.

[14] P. Masarati, V. Muscarello, G. Quaranta, A. Locatelli, D. Mangone, L. Riviello, L. Vigano, "An integrated environment for helicopter aeroservoelastic analysis: the ground resonance case", In Proceedings of the 37th European Rotorcraft Forum, Gallarate, Italy, 2011.

[15] Y.A. Kuznetsov, "Elements of Applied Bifurcation Theory", Springer-Verlag, 1995.

[16] J. Guckenheimer and P. Holmes, "Nonlinear Oscillations, Dynamical Systems and Bifurcations of Vector Fields", Springer, 1993.

[17] E.J. Doedel, A.R. Champneys, T.F. Fairgrieve, Y.A. Kuznetsov, B. Sandstede, X. Wang, "Auto97: Continuation and bifurcation software for ordinary differential equations", A.R.C. Technical Report C.P. No. 101 (14,757), http://indy.cs.concordia.ca/auto/, Sept 2007.

[18] E.J. Doedel, B.E. Oldeman, A.R. Champneys, F. Dercole, T.F. Fairgrieve, Y.A. Kuznetsov, R.C. Paffenroth, B. Sandstede, X.J. Wang, C. Zhang, "Auto-07P: Continuation and bifurcation software for ordinary differential equations", Technical Report, Concordia University, Montreal, Canada, http://indy.cs.concordia.ca/auto/, 2009.

[19] Coetzee, E., Krauskopf, B., and Lowenberg, M., "The Dynamical System Toolbox: Integrating AUTO into MATLAB," The 16th US National Congress of Theoretical and Applied Mechanics, Vol. USNCTAM2010-827, State College, PA, July 2010.

[20] Andrea Bernascone – "Nonlinear Stability Analysis of Helicopter Rotors using Continuation and Bifurcation Methods", Masters Thesis, Politecnico di Milano, 2012.

[21] W. Johnson – "A Comprehensive Analytical Model of Rotorcraft Aerodynamics and Dynamics – Johnson Aeronautics Version, Volume I: Theory Manual", Johnson Aeronautics, 1988.

[22]

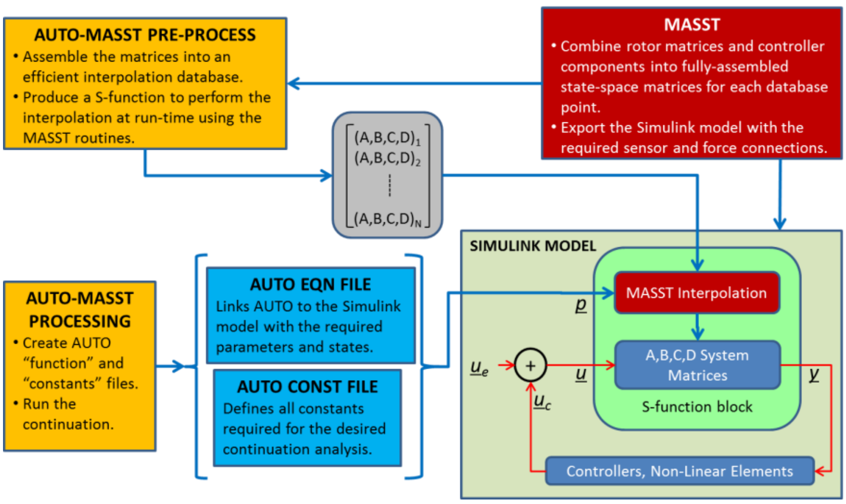

Figure 1: The AUTO-MASST coupling tool, based on reference 4.

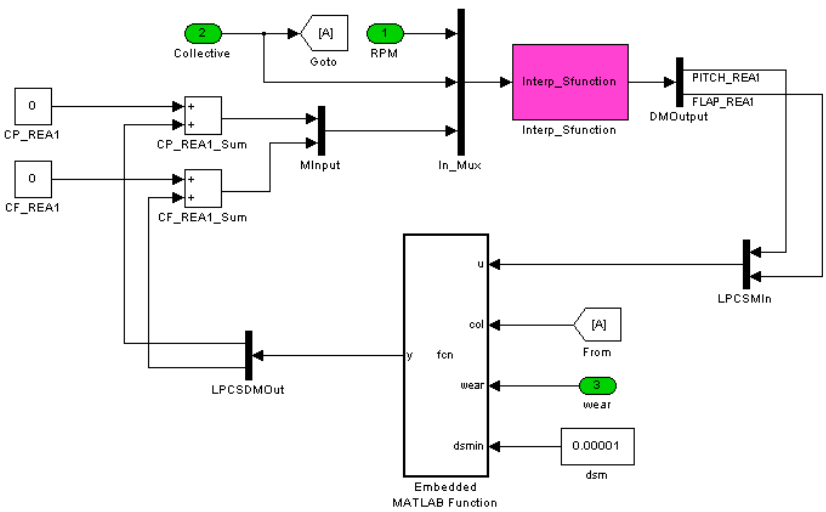

Figure 2: Screenshot of the Simulink model.

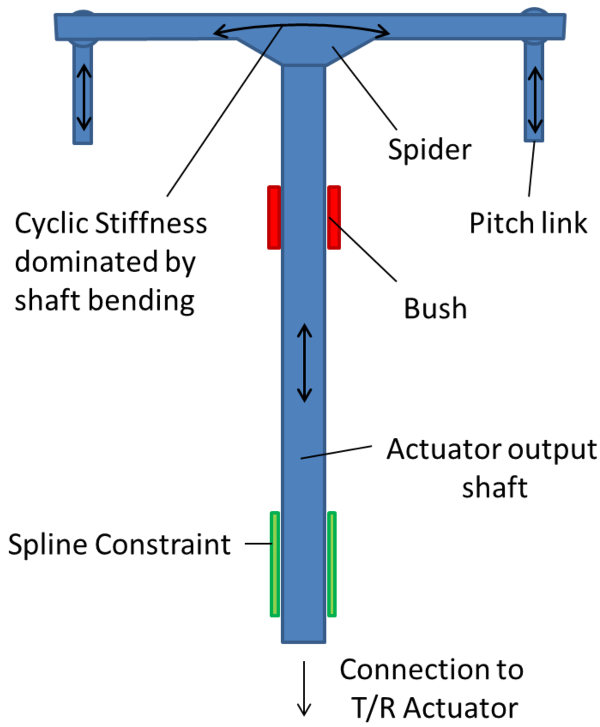

Figure 3: Schematic of the tail rotor control system.

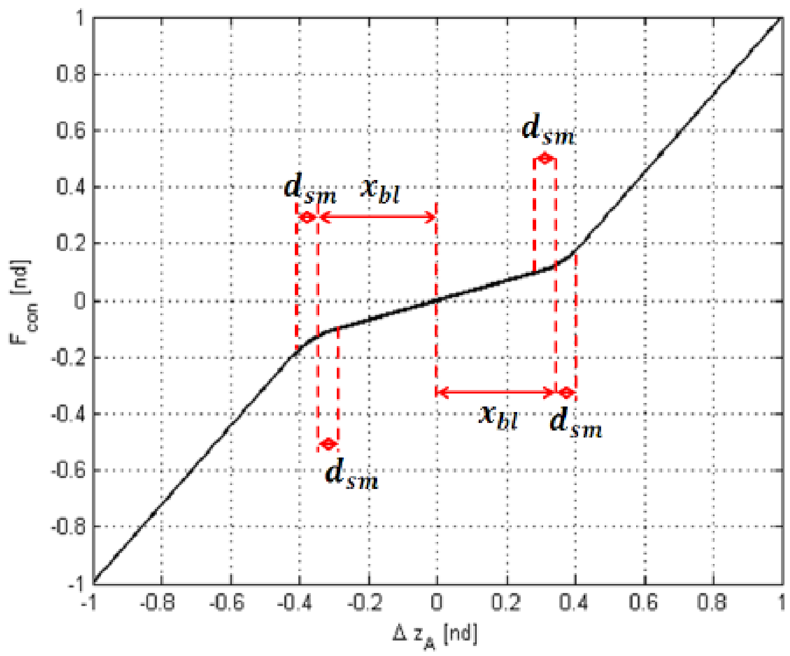

Figure 4: Generalised representation of cyclic control system non-linearity.

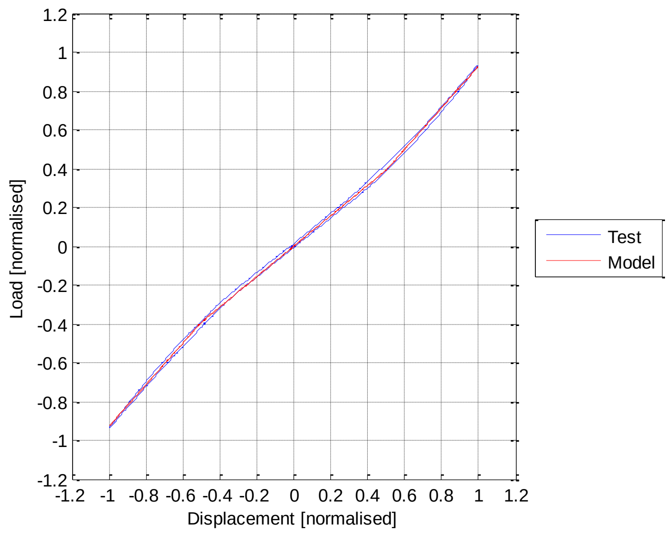

Figure 5: Example of comparison of non-linear control system model to test data, nominal clearance, min collective.

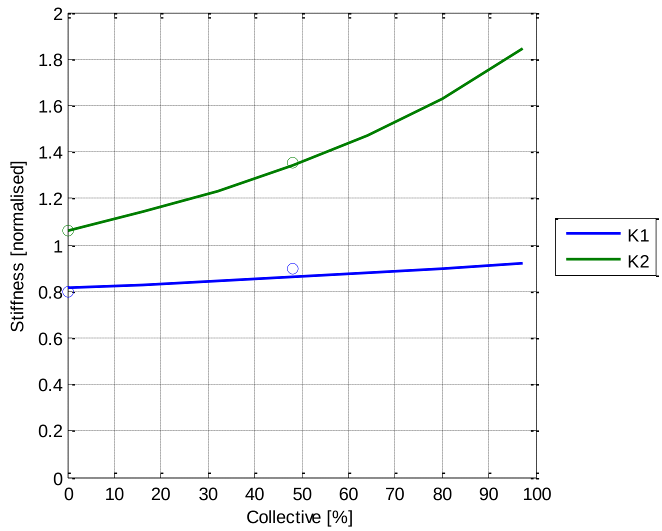

Figure 6: Overall fit of model to the stiffness values obtained from data fitting.

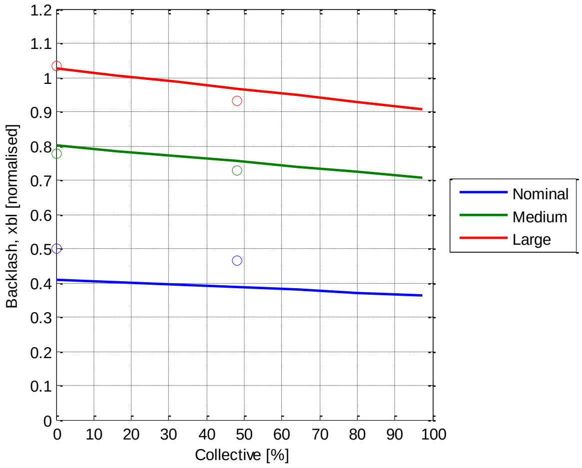

Figure 7: Overall fit of model to the backlash values obtained from data fitting.

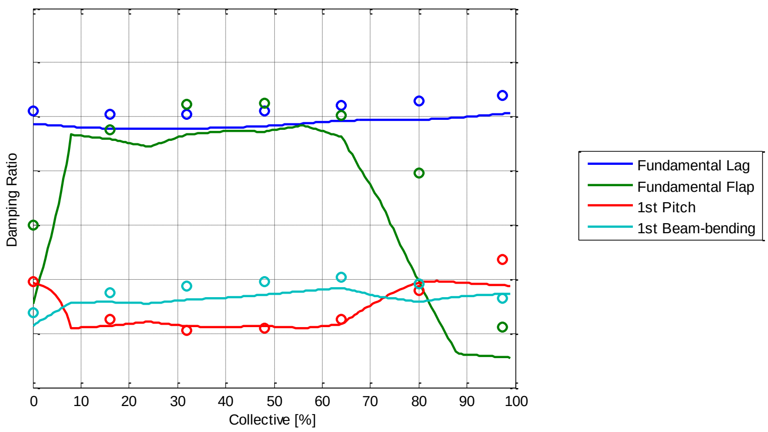

Figure 8: Validation of model versus collective pitch with no bush constraint (stiffness=K_1). Lines are the AUTO-MASST model, markers are CSA.

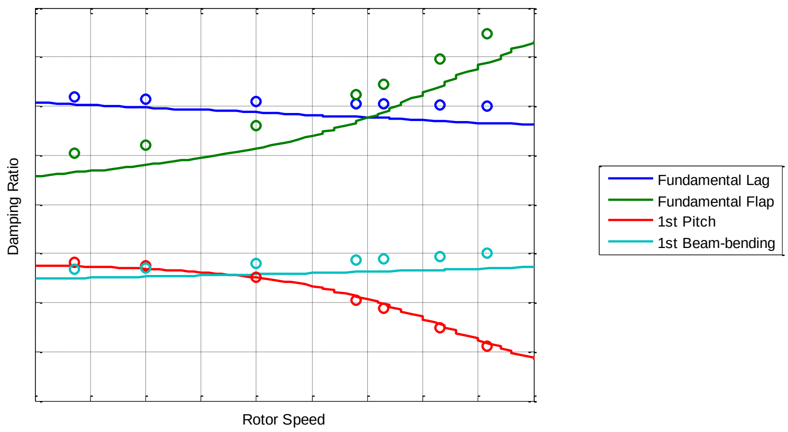

Figure 9: Validation of model versus rotor speed with no bush restraint (stiffness=K_1). Lines are the AUTO-MASST model, markers are CSA.

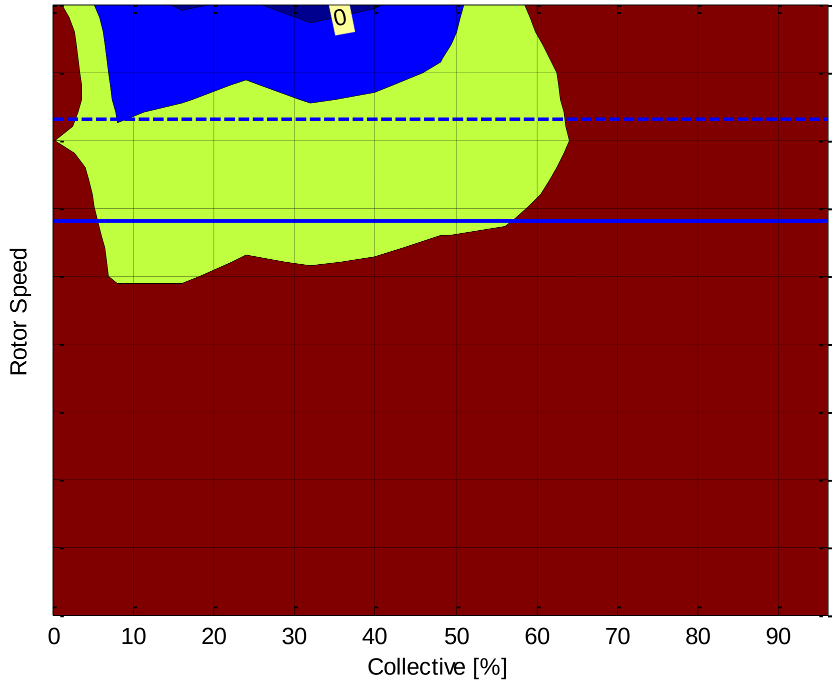

Figure 10: Contours of pitch mode damping ratio with ideal bush restraint, i.e. stiffness = K2. Full blue line shows normal operating rotor speed, dashed blue line shows maximum steady P/OFF rotor speed.

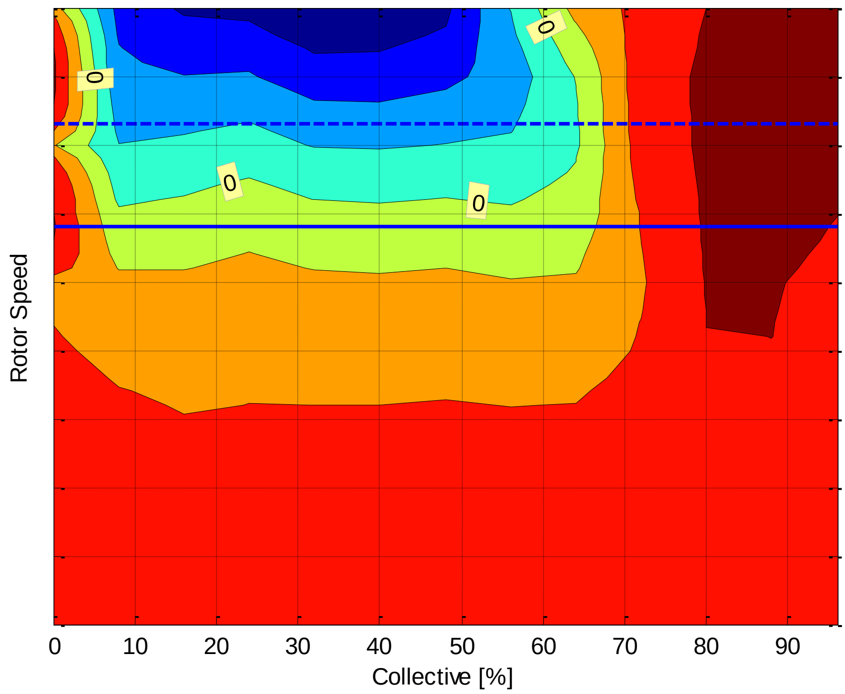

Figure 11: Contours of pitch mode damping ratio on the equilibrium branch (equivalent to linearised damping without the bush restraint, i.e. stiffness = K1). Full blue line shows normal operating rotor speed, dashed blue line shows max steady P/OFF rotor speed.

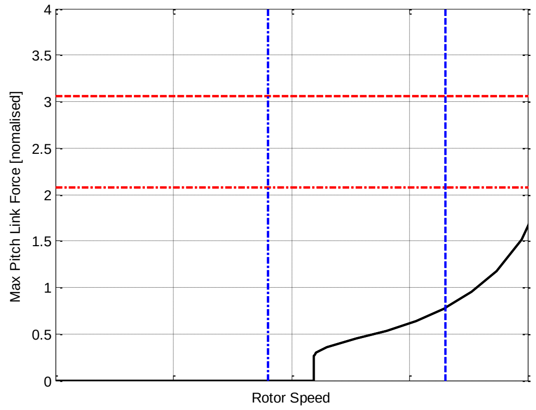

Figure 12: LCO magnitude with nominal (as-manufactured) bush clearance. Blue lines show normal rotor speed (dot-dash) and max steady P/OFF rotor speed (dashed). Red lines show monitor limits for 50hr (dot-dash) and 1hr (dashed).

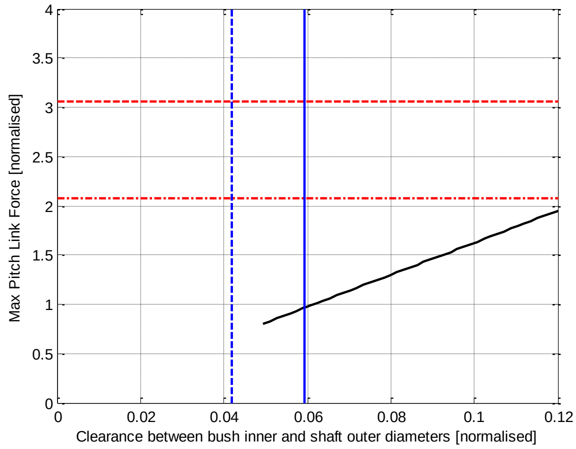

Figure 13: LCO magnitude at max steady P/OFF rotor speed. Blue lines show the minimum (dashed) and maximum (full) acceptable bush clearance. Red lines show monitor limits for 50hr (dot-dash) and 1hr (dashed).

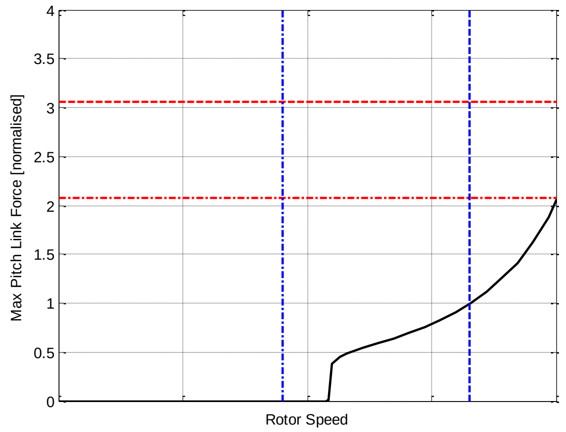

Figure 14: LCO magnitude with maximum acceptable bush clearance. Blue lines show normal NR (dot-dash) and max steady P/OFF NR (dashed). Red lines show monitor limits for 50hr (dot-dash) and 1hr (dashed).